

Article

Dimensioning Models of Optical WDM Rings in Xhaul Access Architectures for the Transport of Ethernet/CPRI Traffic

Vincenzo Eramo ^{1,*} , Marco Listanti ¹, Francesco G. Lavacca ¹ and Paola Iovanna ²

¹ DIET, University of Rome "Sapienza", 00184 Rome, Italy; marco.listanti@uniroma1.it (M.L.); francescogiaccinto.lavacca@uniroma1.it (F.G.L.)

² Ericsson Research, Via Moruzzi 1, 56124 Pisa, Italy; paola.iovanna@ericson.com

* Correspondence: Vincenzo.Eramo@uniroma1.it; Tel.: +39-06-44585372

Received: 23 March 2018; Accepted: 6 April 2018; Published: 12 April 2018



Abstract: The Centralized Radio Access Network (C-RAN) provides a valid solution to overcome the problem of traditional RAN in scaling up to the needed processing resource and quality expected in 5G. The Common Public Rate Interface has been defined to transport traffic flows in C-RAN and recently some market solutions are available. Its disadvantage is to increase by at least 10 times the needed bandwidth and for this reason its introduction will be gradual and will coexist with traditional RAN solutions in which Ethernet traffic is carried towards the radio base stations. In this paper, we propose an Xhaul optical network architecture based on Optical Transport Network (OTN) and Dense Wavelength Division Multiplexing (DWDM) technologies. The network allows for a dynamic allocation of the bandwidth resources according to the current traffic demand. The network topology is composed of OTN/DWDM rings and the objective of the paper is to evaluate the best configuration (number of rings and number of wavelengths needed) to both to minimize the cost and to provide an implementable solution. We introduce an analytical model for the evaluation of the number of wavelengths needed in each optical ring and provide some results for 5G case studies. We show how, although the single ring configuration provides the least cost solution due to the high statistical multiplexing advantage, it is not implementable because it needs switching apparatus with a too high number of ports. For this reason, more than one ring is needed and its value depends on several parameters as the offered traffic, the number of Radio Remote Units (RRU), the percentage of business sub-area and so on. Finally, the analytical model allows us to evaluate the advantages of the proposed dynamic resource allocation solution with respect to the static one in which the network is provided with a number of wavelengths determined in the scenario in which the radio station works at full load. The bandwidth saving can be in the order of 90% in a 5G traffic scenario.

Keywords: 5G; common public rate interface; analytical model; optical networks; dense wavelength; division multiplexing

1. Introduction

In recent years, the evolution of mobile networks into 5G has become the industry focus. 5G will penetrate into almost all areas of our future society. The construction of the user-centric information ecosystem will provide users with extreme service experience. The International Telecommunication Union (ITU) defined three major application scenarios for 5G: Enhanced Mobile Broadband (eMBB), Massive Machine Type Communication (mMTC) and Ultra Reliable Low Latency Communication (uRLLC) [1]. These applications require that 5G bearer networks provide the capability to flexibly and dynamically allocate and release the network resources required by different services, optimize

network connectivity, reduce the costs of the entire network and enhance energy and transport efficiency. Cloud Radio Access Network (C-RAN) or centralized RAN is a technology in which most of the functionalities of a classical e-node of a Long Term Evolution (LTE) network, except the radio ones are centralized and shared in a pool [2]. Traditional C-RANs are organized as a three elements network that contains Base Band Unit (BBU) pool, Radio Remote Unit (RRU) and the network interconnecting BBUs and RRUs called fronthaul [3,4]. The BBU provides baseband signal processing functions and the RRU provides Radio Frequency signal transmission and reception functions. The Common Public Rate Interface (CPRI) [2] has been defined to transport the radio samples between the BBUs and the RRUs through the fronthaul network. The main proposed solutions are: Dark fiber [1,5,6], Passive WDM [1,5], WDM/OTN [7,8], WDM/PON [9,10], and Ethernet [11,12].

The high extension of the fronthaul network leads to two problems: (i) difficulty supporting the real time functionalities of an e-node; and (ii) the high bandwidth cost when pure CPRI solutions are implemented. For this reason, the C-RAN functions are re-split [1]. Instead of two, three functional entities are defined: Centralized Unit (CU), Distributed Unit (DU) and RRU. The CU provides the non-real-time functionalities while the DU provides physical layer functions and the real-time HARQ and ARQ ones. The new fronthaul network is the one between DU and RRU. It is less extensive and that leads to solve the problems before mentioned.

Probably the Ethernet-based technology is the more promising and efficient one but it is not mature yet and needs many investigations. For this reason, we propose and investigate an OTN/WDM-based solution, which is mature and allows for good performance from the delay and jitter point of view.

The objective of this paper is to propose a transport solution for the fronthaul segment based on optical technology that allows for a dynamic bandwidth resource allocation needed to carry the CPRI flows with a consequent saving of bandwidth with respect to a static solution in which the network is provided with bandwidth dimensioned in the worst case when the radio stations are working at full load. The main contributions of this paper are the following:

- We propose a low cost and modular WDM/OTN architecture based on a ring topology; because, in the early developments, C-RAN solutions will coexist with traditional mobile solutions and Radio Base Station (RBS), we define the network architecture so as to support both CPRI and Ethernet traffic.
- We propose a reconfiguration policy of RRUs equipped with smart antennas and implementing Multiple-Input-Multiple-Output (MIMO) techniques; the policy determines the number of antennas to be switched on to support the current traffic.
- An analytical model is introduced for the dimensioning of the number of wavelengths of the optical rings.
- We evaluate the best network configurations (number of optical rings, number of wavelengths, number of RRUs, and . . .) that lead to a low cost solution and supported by the current Dense Wavelength Division Multiplexing (DWDM) technology.
- We evaluate the bandwidth advantages that the introduced transport solution allows us to achieve with respect to the one in which the bandwidth resources are statically allocated in a worst case in which the radio stations are working at full load.

The evolution of the fronthaul network technologies in C-RAN architectures is illustrated in Section 2. The reference scenario considered in our analysis is reported in Section 3. Meanwhile, the dimensioning analytical model of the optical rings is reported in Section 4. The main results are illustrated in Section 5. Finally conclusions and future research items are illustrated in Section 7.

2. Evolution of the Fronthaul Network Technologies in C-RAN Architecture

The C-RAN architecture consists of a considerable number of distributed low-power and low-cost RRUs which are randomly deployed in the network. The RRUs consist of RF transceiver components such as power amplifier, duplexer, and low noise amplifier. Besides, the RRUs help in the conversion of baseband digital signal into RF signal and corresponding up-conversion to the required frequency of

operation. Another component of the C-RAN is the centralized BBUs which are clustered as a BBU pool. It consists of high performance processors as well as real-time (RT) virtualization and management technologies [5]. In addition, the pool aggregates all computational resources and manages a huge number of RRUs located at different antenna sites. A significant advantage of the BBU pooling is that it supports dynamic allocation of the BBU resources to the RRUs to minimize the processing and power consumption. Consequently, it helps significantly in CAPEX reduction. The network interconnecting BBU pool and RRUs is referred to as fronthaul network. A variety of fronthaul technologies can be used in the C-RAN architecture, each with advantages and disadvantages. The main proposed solutions are:

- Dark fiber [1,5,6] illustrated in Figure 1a: It has the advantages of using transmission equipment between BBU and RRU only and provides low latency and simple deployment; the disadvantage is the high use of fiber resources because point-to-point connections have to be established between BBU and RRU.
- Passive WDM [1,5] illustrated in Figure 1b: It uses passive optical multiplexer/demultiplexer to multiplex many wavelengths on an optical fiber. Its advantages are the fiber resource saving and the low power consumption. Its disadvantages are both the cost of colored interfaces in the BBU and RRU and the high accumulated insertion loss that limits the transmission distance. Furthermore, Operation, Administration and Maintenance (OAM) functions are not supported.
- WDM/OTN [7] illustrated in Figure 1c: It allows for the time multiplexing of the CPRI signals on a same wavelength; the solution can save fiber resources, provide OAM functions as well as optical layer and electrical layer performance management and fault detection, provide network protection and ensure high service reliability. The optical bypass of multiplexed CPRI flows allows for low delay that can be even lowered with the introduction of a light OTN [8]. The solution does not need colored interfaces for the wireless equipment. The disadvantage is that the equipment cost is relatively higher and a low cost solution needs to be developed.
- WDM/PON [9,10,13] illustrated in Figure 1d: This technology uses star networks, the fiber resources deployed on the Passive Optical Network (PON) network access layer can be used, and the equipment cost is low.
- Ethernet [11,12] illustrated in Figure 1e: This technology is based on the transport of CPRI flows in Ethernet circuits. the new specification eCPRI [14] has been defining some functional decomposition options and its scope is to enable efficient and flexible radio data transmission via a packet based fronthaul transport network like IP or Ethernet. When RRU switching off [2] and/or CPRI rate reconfigurability [15] techniques are used, this technology allows for resource saving due to the statistical multiplexing advantages. Unfortunately, it does not support the high-precision synchronization needed in CPRI technology and for this reason the IEEE has set up the 802.1 Time-Sensitive Networking (TSN) task group to study the latency-sensitive Ethernet forwarding technology and set up the 1914 Next Generation Fronthaul Interface (NGFI) working group to study CPRI over Ethernet and new Ethernet-based next generation fronthaul interfaces. Some interesting Ethernet-based solutions have been implemented in the Horizon2020 iCirrus project [12] but delay and jitter performance are not provided by the authors. The investigated techniques are preliminary and still in a study phase.

Traditional C-RAN solutions as above have been deemed not adequate because of: (i) the high bandwidth resource consumption in all of the fronthaul segment from the BBUs to the RRUs due to the high bit rate of the CPRI flows; and (ii) the high extension of the fronthaul network that compromises the Hard Automatic Repeat reQuest (HARQ) and Automatic Repeat reQuest (ARQ) real-time functionalities of the mobile network when these functionalities are located in the BBUs. The scientific community is converging towards a solution ad hoc for 5G in which the 5G RAN functions are re-split [1], as illustrated in Figure 2. The original BBU and RRU are reconstructed as three functional entities: Centralized Unit (CU), Distributed Unit (DU) and RRU. The CU mainly provides the non-real-time wireless high-level protocol processing function such as radio resource

management; it can use general hardware platform and be deployed together with mobile edge computing. A DU mainly processes physical layer functions and the real-time HARQ and ARQ ones through a dedicated equipment platform or a general+dedicated hybrid platform. The network segment between the CU and DU is referred to as Midhaul and its bandwidth dimensioning is comparable to the one of the backhaul of traditional mobile networks. The RRU could host the radio functions as well as some physical layer functions to reduce the bandwidth needed between the DU and RRU. The network segment between DU and RRU is the new fronthaul. Its extension is limited with respect to the previous solution and that allows us to overcome the two limitations previously mentioned. The industry has not yet reached a consensus on the standardization of the underlying function division solution between DU and RRU.

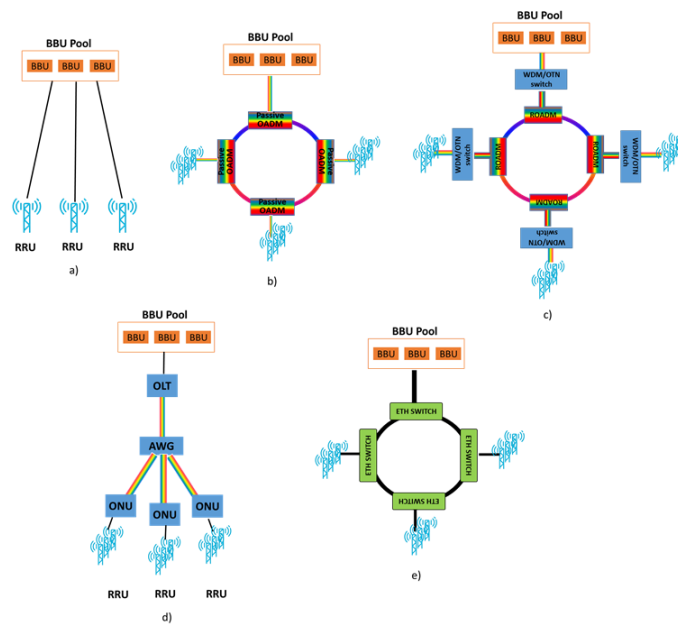


Figure 1. Optional fronthaul network technologies in the C-RAN architecture: dark fiber (a); Passive WDM (b); WDM/OTN (c); WDM/PON (d); and Ethernet (e).

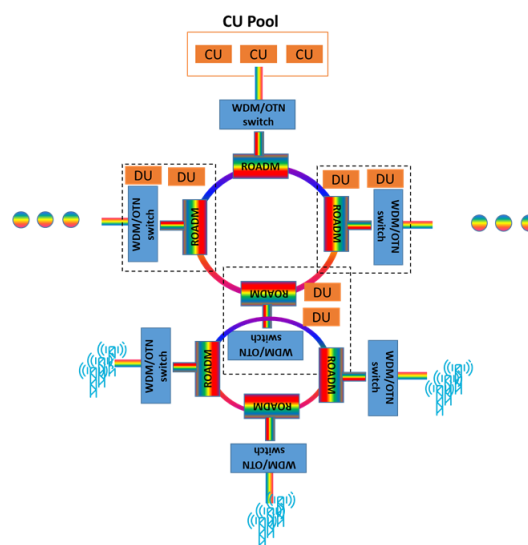


Figure 2. Next generation fronthaul architecture.

The objective of this paper is to propose and investigate the performance of a fronthaul network based on OTN/WDM transport technology. The proposed solution allows for a dynamic bandwidth allocation. We introduce an analytical model to evaluate the advantages of the proposed solution with respect to a static bandwidth allocation strategy.

3. Reference Scenario

The reference scenario is shown in Figure 3. RRUs and RBSs are connected to both Ethernet switches and a DU pool through a WDM/OTN transport network with a given number of optical rings. The Ethernet switches and the DU pool are located in a Central Office (CO). The main components of the network architecture are:

- Access Switch (AS): It is composed of one Reconfigurable Optical Add Drop Multiplexing (ROADM) and a WDM/OTN switch; the WDM/OTN switch frames/de-frames in OTN frames the CPRI and Ethernet flows coming from/directed to the RRUs and RBSs, respectively. The OTN/WDM switch is also equipped with transceivers able to generate/receive colored wavelengths that are added/dropped by an ROADMs. The use of an ROADM guarantees transparently routing wavelengths that are only generated from/received by other ASs and directed to/coming from the WDM/OTN HUB.
- WDM/OTN HUB: It handles the generated/received traffic by the Ethernet switches and the DU pool; it performs framing/de-framing of the Ethernet and CPRI flows in/from OTN frames; it is equipped with WDM interfaces to generate the colored wavelengths in which to carry the OTN frames; and it forwards/receives the WDM signal to/from the right optical ring.

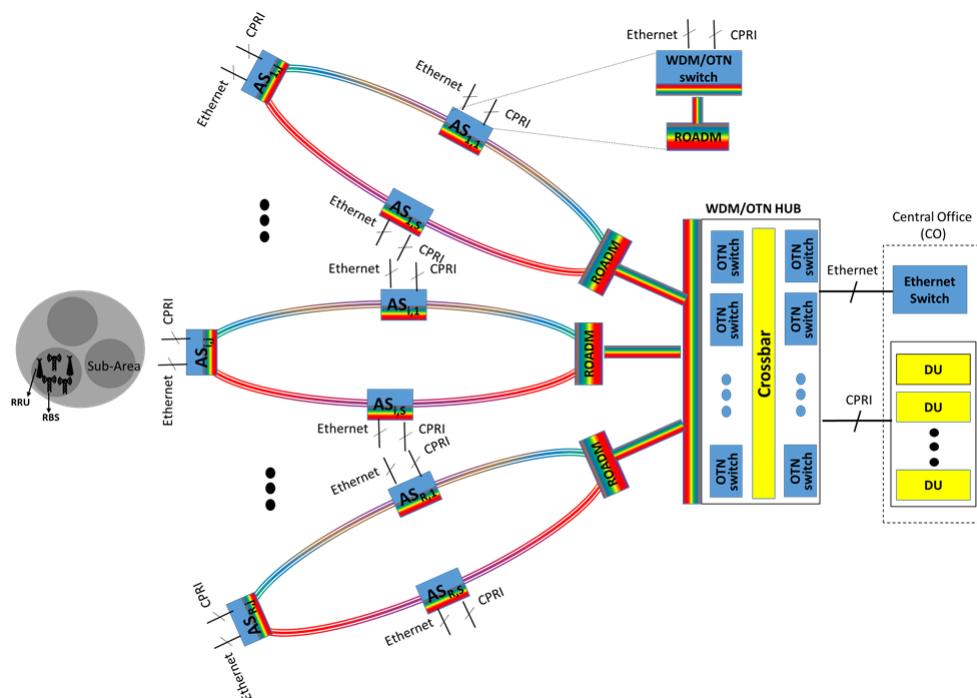


Figure 3. Reference scenario. RRUs and RBSs are connected to ethernet switches and a DU poll through a WDM/OTN transport network.

Recently proposed architectural and technological solutions help to realize low delay and cost-effective WDM/OTN transport networks. Among them:

- The definition of scalable WDM/OTN HUB architectures organized in three stages: the first and third stage are equipped with small size OTN switches while the second one is equipped with a spatial crossbar matrix [16,17].
- The definition of a light OTN framing [8] allows for a reduction of the overhead introduced to perform the Forward Error Code (FEC) operation [8]; some experiments have shown a FEC latency lower than 4 μ s with no appreciable degradation of the FEC gain with respect to the traditional OTN case.
- A photonic integration technology allows for cost-effective realization of the ROADMs and transceivers [8]; in particular, silicon photonics are most suitable for large-scale integrated switching devices due to its characteristics of easy integration with control electronics, high miniaturization, mass producibility and low cost due to the use of a well-established Complementary Metal Oxide Semiconductor (CMOS) production infrastructure. Concerning integrated multiwavelength transceivers, relevant technological advances have been made with two different technological approaches that lead to InP monolithic-integrated DWDM transceivers and silicon photonics-based transceivers [18,19].

To reduce as much as possible the bandwidth consumption, we employ the reconfiguration capability of the WDM/OTN transport network and adapt the bandwidth resources to the current traffic; in particular, we employ the capacity of changing the CPRI flow rate according to the current traffic handled by any RRU. That could be realized in the case in which the RRUs are equipped with a given number of MIMO smart antennas [15] that are activated according to the traffic amount to be handled. In such a way, the bit rates of the CPRI flows are changed and the needed bandwidth is re-allocated.

The objective of this paper is to evaluate the best configuration of the proposed OTN/WDM architecture in terms of number of optical rings, number of ASs, number of wavelengths, and percentage of used RRUs with the aim at getting a low solution and supported with the current DWDM technology. We also evaluate the advantages of the proposed solution with respect to a static resource allocation solution in which the network resources are dimensioned when the radio stations are working at full load.

To perform the evaluation, we need to introduce an analytical model for the dimensioning of the number of wavelengths needed in the optical rings as a function of the main traffic and network parameters.

4. Dimensioning Analytical Model for the Optical Rings

We evaluate the number of wavelengths needed in each optical ring under the following assumptions:

1. A reference area is considered subdivided in a given number of sub-areas where RRUs and RBSs handle the user traffic. We also assume that each Access Switch handles D sub-areas. The maximum user traffic capacity that the RBS can handle is denoted with C_{RBS} . We also assume that the installed RBSs are always turned on and provides a basic capacity for the coverage of any sub-area. The RRUs provide additional capacity needed in the intervals in which the traffic increases. The RRUs are only used when the basic capacity provides by the RBSs is not sufficient to support the user traffic.
2. Each RRU implements a MIMO technological solution with the possibility of Q configurations denoted as S_0, S_1, \dots, S_{Q-1} . We assume that switching off and switching on of antennas is performed when traffic variation occurs; in particular when the configuration S_i ($i = 0, \dots, Q - 1$) is activated, n_i ($i = 0, 1, \dots, Q - 1$) antennas are turned on with the capacity of handling a user traffic capacity C_i^{RRU} ($i = 0, \dots, Q - 1$); let f_i^{CPRI} ($i = 0, \dots, Q - 1$) denote the bit rate of the CPRI flow generated/received when the RRU is in the configuration S_i ($i = 0, \dots, Q - 1$). We order the configurations in increasing order of the bit rate of the CPRI flows.

3. R two fibers optical rings are considered. Each optical ring is provided with S ASs. The generic AS is referred to as $AS_{i,j}$ that denotes the j -th AS ($j = 1, \dots, S$) in the i -th ($i = 1, \dots, R$) optical ring. We denote with L^i the set of the links in the i -th optical ring.
4. The traffic is cycle-stationary with N stationary periods and our traffic modeling is inherited from [20]; for instance, N equals 24 when the classical daily traffic variation has to be reproduced. The user peak traffic generated in the sub-areas handled by an AS can follow one of two profiles corresponding to business and residential traffic. The business and residential profiles occur with probability p_b and p_r , respectively, with obviously $p_b + p_r = 1$. The user peak traffic generated in the sub-areas, expressed in Gbps, are independent and identically distributed (i.i.d.) variables; therefore, the upstream (downstream) user peak traffic generated in any business sub-area in the k -th stationary interval is characterized by a variable $A_k^{u,b}$ ($A_k^{d,b}$) that, according to [20], we assume log-normal distributed of parameters $(\mu_k^{u,b}(\mu_k^{d,b}), \sigma_k^{u,b}(\sigma_k^{d,b}))$. For the residential sub-areas, we have the log-normal variables $A_k^{u,r}$ ($A_k^{d,r}$) of parameters $(\mu_k^{u,r}(\mu_k^{d,r}), \sigma_k^{u,r}(\sigma_k^{d,r}))$.
5. The number of RRUs and RBSs are dimensioned in each sub-area to support the peak offered traffic and by applying the procedure reported in [2]; let us denote with n_{RRU}^b (n_{RRU}^r) and n_{RBS}^b (n_{RBS}^r) the number of RRUs and RBSs installed in a business (residential) sub-area, respectively, when the dimensioning procedure is applied.
6. A routing algorithm characterized by the variables $x_l^{u,i,j}$ ($x_l^{d,i,j}$) assumes the value 1 if the traffic between the $AS_{i,j}$ (CO) and the CO ($AS_{i,j}$) is routed on the link $l \in L^i$; otherwise, its value is 0.
7. The resources (wavelengths) carrying Ethernet and CPRI flows, respectively, are separated and no wavelength can carry both Ethernet and CPRI flows.
8. OTN/WDM switches do not perform any grooming operation.

The meaning of the all parameters and variables used are reported in Tables 1 and 2, respectively.

If we denote with $w_l^{(i),k}$ the number of wavelengths needed on the link $l \in L^i$ in the i -th optical ring and in the k -th ($k \in [0..N - 1]$) Stationary Interval (SI), we can express the number $n_w^{(i)}$ of wavelengths needed for the i -th optical ring as follows:

$$n_w^{(i)} = \max_{k \in [0..T-1]} \max_{l \in L^i} w_l^{(i),k} \tag{1}$$

Due to Assumptions 6 and 7, the number $n_w^{(i)}$ of wavelengths is given by the sum of wavelengths needed to carry the Ethernet and CPRI flows between the tuples $(AS_{i,j}, CO)$ ($j = 1, \dots, S$) and $(CO, AS_{i,j})$ ($j = 1, \dots, S$) and that use the link l in their routing path. We can simply write:

$$w_l^{(i),k} = \sum_{p \in \{u,d\}} \sum_{j=1}^S x_l^{p,i,j} (n_{\lambda,Eth}^{p,i,j,k} + n_{\lambda,CPRI}^{p,i,j,k}) \tag{2}$$

where $n_{\lambda,Eth}^{u,i,j,k}$ ($n_{\lambda,Eth}^{d,i,j,k}$) and $n_{\lambda,CPRI}^{u,i,j,k}$ ($n_{\lambda,CPRI}^{d,i,j,k}$) denote the number of wavelengths needed to carry the Ethernet and CPRI flows in the k -th SI between $AS_{i,j}$ (CO) and CO ($AS_{i,j}$), respectively. We show in Sections 4.1 and 4.2 the evaluation of $n_{\lambda,Eth}^{u,i,j,k}$ and $n_{\lambda,CPRI}^{u,i,j,k}$, respectively. The evaluation of $n_{\lambda,Eth}^{d,i,j,k}$ and $n_{\lambda,CPRI}^{d,i,j,k}$ can be performed in a similar way.

4.1. Evaluation of $n_{\lambda,Eth}^{u,i,j,k}$

To evaluate the values $n_{\lambda,Eth}^{u,i,j,k}$ ($k = 0, \dots, N - 1$), we start by the knowledge of the statistical of the variable $N_{AS_{i,j},Eth}^k$, denoting the number of GEthernet flows to be carried between the sub-area $AS_{i,j}$ and the CO in the k -th SI. We show in Appendix A how it is possible to evaluate the probabilities $P_{N_{AS_{i,j},Eth}^k}^j$ ($j = 0, 1, \dots, Dn_{RBS} C_{RBS}$) of the random variable $N_{AS_{i,j},Eth}^k$.

Let η_{Eth} denote the maximum number of GEthernet flows that is possible carry on any wavelength. Obviously, η_{Eth} depends on both the wavelength bandwidth and the OTN containers in which the Ethernet flows are mapped [21].

We will choose $n_{\lambda, Eth}^{u,i,j,k}$ as the α -th percentile of the needed number $\frac{N_{AS_{i,j}, Eth}^k}{\eta_{Eth}}$ of wavelengths, that is:

$$n_{\lambda, Eth}^{u,i,j,k} \text{ is chosen as the smallest value } x \text{ such that } Pr\left(\frac{N_{AS_{i,j}, Eth}^k}{\eta_{Eth}} > x\right) < 1 - 0.01 \cdot \alpha \quad (3)$$

The value of α is chosen very low to guarantee that the wavelengths are always available to carry Ethernet flows.

4.2. Evaluation of $n_{\lambda, CPRI}^{u,i,j,k}$

Let us introduce the following events and probabilities:

- \mathcal{E}_{S_h} : It denotes the event that the RRU's of the sub-area handled by $AS_{i,j}$ active the MIMO configuration S_h ($h = 0, \dots, Q - 1$) with n_h ($h = 0, \dots, Q - 1$) active antennas; $p_{S_h, k} = Pr(\mathcal{E}_{S_h})$ denotes the probability of the event \mathcal{E}_{S_h} in the k -th SI; the probabilities $p_{S_h, k}$ ($h = 0, \dots, Q - 1$; $k = 0, \dots, N - 1$) are evaluated in Appendix B.
- $\mathcal{E}_{r_0, \dots, r_{Q-1}}^S$: It denotes the joint event that r_h sub-areas handled by $AS_{i,j}$, for $h = 0, \dots, Q - 1$, active the configuration S_h ; $p_{r_0, \dots, r_{Q-1}}^{S, k}$ denotes the probability of the event in the k -th SI; due to the statistical independence (Assumption 4) mentioned above, we can express $p_{r_0, \dots, r_{Q-1}}^{S, k}$ as follows:

$$p_{r_0, \dots, r_{Q-1}}^{S, k} = \binom{D}{r_0} \binom{D - r_0}{r_1} \dots \binom{D - \sum_{h=0}^{Q-3} r_h}{r_{Q-2}} p_{S_0, k}^{r_0} \dots p_{S_{Q-1}, k}^{r_{Q-1}} \quad (4)$$

The introduction of these above events allows for the evaluation of the probabilities of the random variable $N_{AS_{i,j}, CPRI}^k$ that denotes the number of wavelengths needed to carry CPRI flows from $AS_{i,j}$ to the CO in the k -th SI. We can simply write:

$$Pr(N_{AS_{i,j}, CPRI}^k = h) = \sum_{(r_0 \dots r_{Q-1}) / \sum_{h=0}^{Q-1} r_h = D} I(F^\lambda(r_0, \dots, r_{Q-1}) = h) p_{r_0, \dots, r_{Q-1}}^{S, k} \quad (5)$$

where $I(*)$ is the indicator function and $F^\lambda(r_0, \dots, r_{Q-1})$ is a function that establishes the number of wavelengths needed to support $r_h n_{RRU}$ CPRI flows at bit rate f_h^{CPRI} for $h = 0, \dots, Q - 1$. The function $F^\lambda(*)$ depends on type of mapping and multiplexing chosen for the OTN transport network. We assume the adoption of OTN multiplexing with at most two layers in which the CPRI flows are multiplexed in ODU2 [22] and ODU2's are multiplexed in a high level container transmitted on the wavelength; let η_h^{CPRI} ($h = 0, \dots, Q - 1$) denote the maximum number of CPRI flows into one ODU2 generated by RRU's configured according to MIMO configuration S_h ($h = 0, \dots, Q - 1$). If η^λ denotes the maximum number of ODU2s into a wavelength, we can express $F^\lambda(r_0, \dots, r_{Q-1})$ as follows:

$$F^\lambda(r_0, \dots, r_{Q-1}) = \frac{\sum_{h=0}^{Q-1} \lceil \frac{r_h n_{RRU}}{\eta_h^{CPRI}} \rceil}{\eta^\lambda} \quad (6)$$

Finally, we choose $n_{\lambda, CPRI}^{u,i,j,k}$ as the α -th percentile of the needed number $N_{AS_{i,j}, CPRI}^k$ of wavelengths, that is:

$$n_{\lambda, CPRI}^{u,i,j,k} \text{ is chosen as the smallest value } x \text{ such that } Pr(N_{AS_{i,j}, CPRI}^k > x) < 1 - 0.01 \cdot \alpha \quad (7)$$

Table 1. Radio station, OTN/WDM network and traffic parameters.

Q	Number of MIMO Configurations for each RRU	n_i	Number of active antennas for the MIMO Configuration S_i ($i = 0, \dots, Q - 1$)
C_i^{RRU}	RRU User Capacity (Mbps) for the MIMO Configuration S_i ($i = 0, \dots, Q - 1$)	f_i^{CPRI}	CPRI bit rate (Gbps) for the MIMO Configuration S_i ($i = 0, \dots, Q - 1$)
C_{RBS}	RRU User Capacity (Mbps)	n_{RRU}^b	Number of RRUs in a business sub-area
n_{RBS}^b	Number of RBSs in a business sub-area	n_{RRU}^r	Number of RRUs in a residential sub-area
n_{RBS}^r	Number of RBSs in a residential sub-area	D	Number of sub-areas handled by each AS
R	Number of Optical Rings	S	Number of Access Switches in each Optical Ring
L^i	Set of the links in the i -th Optical Ring	η_i^{CPRI}	Maximum number of CPRI flows carried in one ODU2 for the MIMO Configuration S_i ($i = 0, \dots, Q - 1$)
η^λ	Number of ODU2s in a wavelength	η_{Eth}	Number of Ethernet flows carried on any wavelength
N	Number of Stationary Intervals (SI)	p_b	Probability of a business sub-area
p_r	Probability of a residential sub-area	$(\mu_k^{u,b}, \sigma_k^{u,b})$	Log-normal distribution parameters for the upstream traffic in a business sub-area
$(\mu_k^{d,b}, \sigma_k^{d,b})$	Log-normal distribution parameters for the downstream traffic in a business sub-area	$(\mu_k^{u,r}, \sigma_k^{u,r})$	Log-normal distribution parameters for the upstream traffic in a residential sub-area
$(\mu_k^{d,r}, \sigma_k^{d,r})$	Log-normal distribution parameters for the downstream traffic in a residential sub-area	$A_{o,b}$	Peak average traffic in the PHI parameters for the upstream in a business sub-area
$A_{o,r}$	Peak average traffic in the PHI parameters for the upstream in a residential sub-area		

Table 2. Variables.

$w_l^{(i),k}$	Number of wavelengths needed in the link l of the i -th Optical Ring and in the k -th SI	$n_w^{(i)}$	Number of wavelengths needed for the i -th Optical Ring
$x_l^{p,i,j}$	It assumes value 1 if the CPRI and CPRI flows from $AS_{i,j}$ to CO ($p = u$) or from CO to $AS_{i,j}$ ($p = d$) are routed on link l ; otherwise its value is 0	$n_{\lambda,Eth}^{p,i,j,k}$	Number of wavelengths needed to carry Ethernet flows in the k -th SI from $AS_{i,j}$ to CO $AS_{i,j}$ or from CO to $AS_{i,j}$ ($p = d$)
$n_{\lambda,CPRI}^{p,i,j,k}$	Number of wavelengths needed to carry Ethernet flows in the k -th SI from $AS_{i,j}$ to CO $AS_{i,j}$ or from CO to $AS_{i,j}$ ($p = d$)	$N_{AS_{i,j},Eth}^k$	Number of Ethernet flows (random variable) to be carried from $AS_{i,j}$ to CO in the k -th SI
$N_{AS_{i,j},CPRI}^k$	Number of CPRI flows (random variable) to be carried from $AS_{i,j}$ to CO in the k -th SI		

5. Numerical Results

Next, we report some dimensioning results to verify the effectiveness of the proposed solution in reducing the number of wavelengths used. We also verify the impact that the offered traffic amount and type (business and residential) and the transport network topology (i.e., number of optical rings) have on the wavelength dimensioning.

We consider an area of 1 km² handled by a central office that contains a DU pool and Ethernet switches. We assume that the area is divided into $T = 200$ squared sub-areas and each sub-area is covered with a given number of RRUs and RBSs that generate CPRI and GEthernet flows, respectively.

We assume that the traffic offered to each sub-area is cycle-stationary with $N = 24$ stationary intervals modeling the daily traffic trend. The peak traffic offered to any sub-area is distributed according to a log-normal distribution [20] whose mean value depends on the SI considered, the considered region (business and residential) and the traffic direction (upstream and downstream). The average peak traffic normalized to the average peak traffic during the Peak Hour Interval (PHI) is reported in Figure 4 for the business and residential regions [23,24].

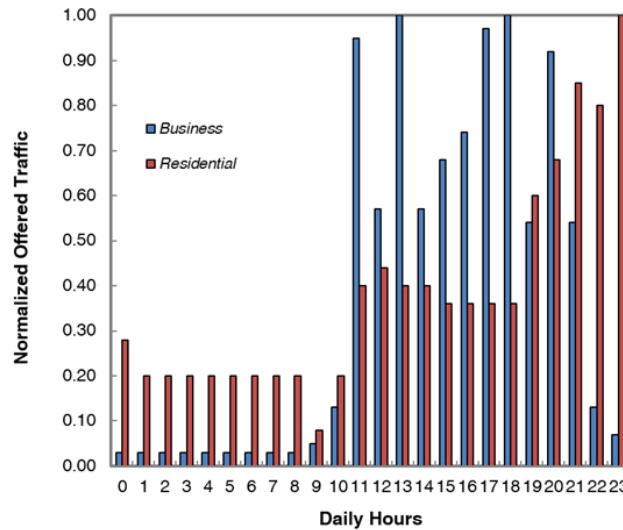


Figure 4. Normalized traffic profile for business and residential sub-area.

We assume that the upstream traffic is 70% of the downstream one. We also denote with $A_{o,b}$ and $A_{o,r}$ the average peak traffic in the PHI for business and residential regions, respectively. Finally, the parameters of the log-normal distribution are chosen so as to guarantee for the distribution matching of both the forecast average peak traffic and a typical standard deviation equal to 0.25 [20].

To support the user traffic, the number of RRUs and RBSs installed in each sub-area are dimensioned according to the procedure illustrated in [2]. Let γ denote the ratio of the number n_{RRU}^x ($x \in \{b, r\}$) of RRUs to the total number $n_{RRU}^x + n_{RBS}^x$ ($x \in \{b, r\}$) of radio stations. To achieve the required flexibility and cost efficiency, eleven different line bit rates of CPRI flows (Options 1–10 and 7a) have been defined [25]. As an example, we consider only Options 2–3, 5 and 7 that allow for the transport of radio samples of signals usually generated in mobile systems. We assume a radio bandwidth equal to 20 MHz and $Q = 5$ possible configurations for any RRU where the configuration S_0 corresponds to the switched off RRU. In particular the active number of antennas is $n_0 = 0$, $n_1 = 1$, $n_2 = 2$, $n_3 = 4$ and $n_4 = 8$ for the configurations S_0, S_1, S_2, S_3 , and S_4 , respectively. The capacity of an RRU for these values of antennas is $C_0^{RRU} = 0$, $C_1^{RRU} = 75$ Mbps, $C_2^{RRU} = 150$ Mbps, $C_3^{RRU} = 300$ Mbps and $C_4^{RRU} = 600$ Mbps to which correspond the CPRI bit rates of the flow generated/received $f_0^{CPRI} = 0$, $f_1^{CPRI} = 1.2288$ Gbps, $f_2^{CPRI} = 2.4576$ Gbps, $f_3^{CPRI} = 4.8152$ Gbps and $f_4^{CPRI} = 9.8304$ Gbps [22]. An ODU2 container can carry a maximum number of $\eta_0^{CPRI} = 0$, $\eta_1^{CPRI} = 8$, $\eta_2^{CPRI} = 4$, $\eta_3^{CPRI} = 2$ and $\eta_4^{CPRI} = 1$ CPRI flows of the antenna configurations S_0, S_1, S_2, S_3 , and S_4 respectively [22]. The number of active antennas, the RRU capacities, the CPRI bit-rates and the maximum number of CPRI flows carried in one ODU2 for configurations S_1, S_2, S_3 , and S_4 are reported in Table 3. Finally, RBSs are also employed with capacity $C_{RBS} = 600$ Mbps.

Table 3. Number of active antennas, RRU capacities, CPRI bit-rates and maximum number of CPRI flows carried in one ODU2 for the antenna configurations S_1 , S_2 , S_3 and S_4 .

	S_1	S_2	S_3	S_4
Number of active antennas	1	2	4	8
RRU Capacity	75 Mbps	150 Mbps	300 Mbps	600 Mbps
CPRI bit-rate	1.2288 Gbps	2.4576 Gbps	4.9152 Gbps	9.8304 Gbps
Number of CPRI flows in one ODU2	8	4	2	1

We consider optical rings in which each wavelength carries a 100 Gbps flow that leads to have $\eta^\lambda = 10$. Shortest paths are selected for routing the traffic demands between any tuple AS-CO (CO-AS).

We evaluate the effectiveness of the proposed network reconfiguration solution in Figures 5 and 6 where we report the total number of wavelengths used and the number of wavelengths used in each optical ring, respectively, as a function of the used RRU percentage γ . The average peak traffic in the PHI is chosen equal to $A_{o,b} = 26$ Gbps and $A_{o,r} = 16$ Gbps for business and residential sub-area, respectively. In particular, the values shown in Figure 5 measure the cost of the solutions considered. We also compare the dimensioning results achieved by applying the proposed dynamic resource allocation solution to a static one in which the optical rings are statically dimensioned that is when the network provides the sufficient bandwidth to carry the traffic flows generated by the RRUs and RBSs in full load condition with all of the antennas active. We consider a study case in which the number R of optical rings is varied and chosen equal to 1, 2 and 4 and each of them interconnects $S = 10$ Access Switches. The variation of the number of optical rings leads to changing the number $D = \frac{T}{RS}$ of sub-areas handled by any AS from 20 to 5 for R varying from 1 to 4, respectively. From the results reported in Figure 5, we can notice how the proposed dynamic resource allocation solution allows for remarkable saving with respect to the static solution in which the bandwidth resources are not shared and dimensioned according to the worst case, that is in the case in which the installed hardware is operating at full load. As an example, when $R = 1$ and $\gamma = 0.6$ the static and dynamic solutions need a number of wavelengths equal to 960 and 92 wavelengths, respectively, and consequently the cost saving is in the order of 90%. In Figure 5, we can also observe how the use of fewer rings leads to using fewer wavelengths, which is due to the higher number of sub-area handled by each AS with the consequence of a higher statistical multiplexing gain. For instance, in the case $\gamma = 0.7$, the total number of wavelengths needed equals 130, 210 and 350 for R equal to 1, 2 and 4, respectively. The problem of fewer rings may lead to solutions that not can be implemented (i.e., ROADMs or transmission systems technology not available due to the high number of wavelengths needed) and for this reason a right trade-off has to be chosen between costs and feasibility. For instance, in our example, in the case in which 128 wavelengths can be supported at 100 Gbps rate, the best solution is the one with two optical rings each one supporting 105 wavelengths as illustrated in Figure 6.

The impact of the traffic type (business and residential) on the dimensioning is investigated in Figures 7 and 8 where we report the number of wavelengths per optical ring as a function of the probability that any sub-area handles residential user traffic. The results reported in Figure 7 are obtained by varying the used RRU percentage from 0% to 100%. We consider a network organized in two optical rings. The other parameter values are chosen as the ones of Figures 5 and 6. We can observe how the wavelength dimensioning does not depend only on the values of peak average traffic $A_{o,b}$ and $A_{o,r}$ but even on the percentage of residential and business sub-area. Because the peak average traffic in the PHI occurs in different stationary intervals for business and residential sub-areas, respectively, then the bandwidth sharing between business and residential users may lead to less severe dimensioning. For instance in the case $\gamma = 1$, the lowest dimensioning occurs for $p_r = 0.80$ when 309 wavelengths are needed. That is confirmed in Figure 8 where we have chosen the residential peak traffic $A_{o,r}$ equal to 16 Gbps and varied the ratio $\omega = \frac{A_{o,b}}{A_{o,r}}$ from 0.5 to 2.

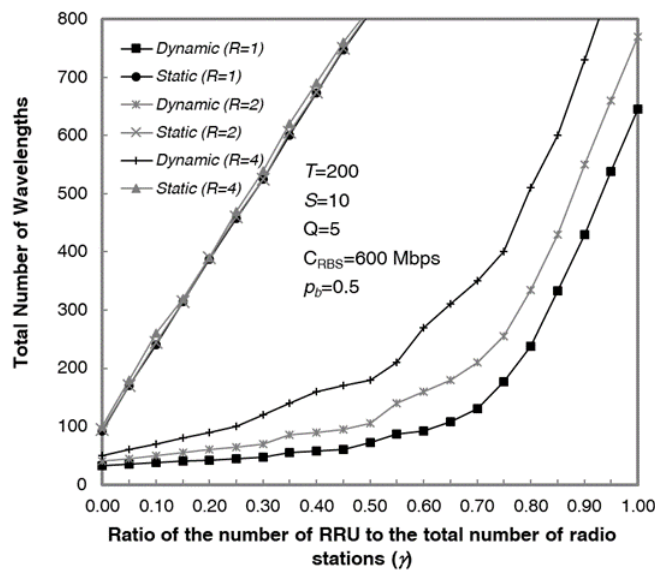


Figure 5. Comparison of the total number of wavelengths for the static and dynamic scenario cases. The total number of wavelengths is reported as a function of the used RRU percentage in the case of number R of optical rings equal to 1, 2 and 4. The residential and business sub-area probabilities p_r and p_b are chosen equal to 0.5 and their peak offered traffic in the PHI are $A_{o,b} = 26$ Gbps and $A_{o,r} = 16$ Gbps. The reference area is composed of $T = 200$ sub-areas and each optical ring interconnects $S = 10$ Access Switches, each one handling the traffic of $D = \frac{T}{SR}$ sub-areas. Each RRU can chose one of $Q = 5$ MIMO configurations according to the offered traffic. The configurations provide the user capacities $C_0^{RRU} = 0$, $C_1^{RRU} = 75$ Mbps, $C_2^{RRU} = 150$ Mbps, $C_3^{RRU} = 300$ Mbps and $C_4^{RRU} = 600$ Mbps and generate CPRI traffic flows at bit rate $f_0^{CPRI} = 0$ Gbps, $f_1^{CPRI} = 1.2288$ Gbps, $f_2^{CPRI} = 2.4576$ Gbps, $f_3^{CPRI} = 4.8152$ Gbps and $f_4^{CPRI} = 9.8304$ Gbps, respectively. An OTN with two layers (ODU2 and ODU4) is considered with wavelengths carrying 100 Gbps flows.

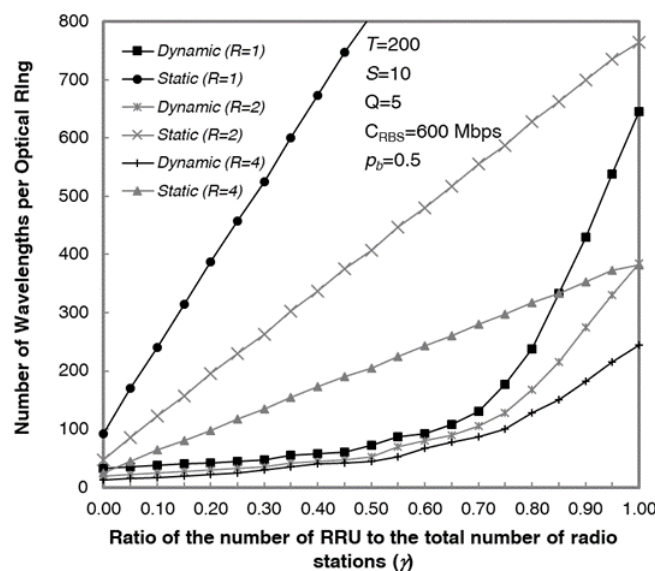


Figure 6. Comparison of the number of wavelengths per optical ring for the static and dynamic scenario cases. The number of wavelengths per optical ring is reported as a function of the used RRU percentage γ in the case of number R of optical rings equal to 1, 2 and 4. The values of the other parameters are chosen as the ones in Figure 5.

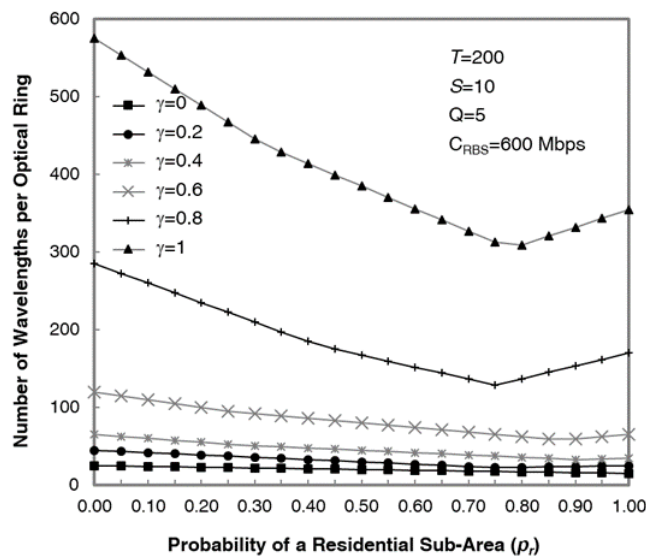


Figure 7. The number of wavelengths per optical ring is reported as a function of the probability p_r of residential sub-area. The percentage γ of used RRUs is varied from 0 to 1. The peak offered traffic is $A_{o,b} = 26$ Gbps and $A_{o,r} = 16$ Gbps for business and residential sub-area, respectively. $R = 2$ optical rings are considered. The values of the other parameters are chosen as the ones in Figure 5.

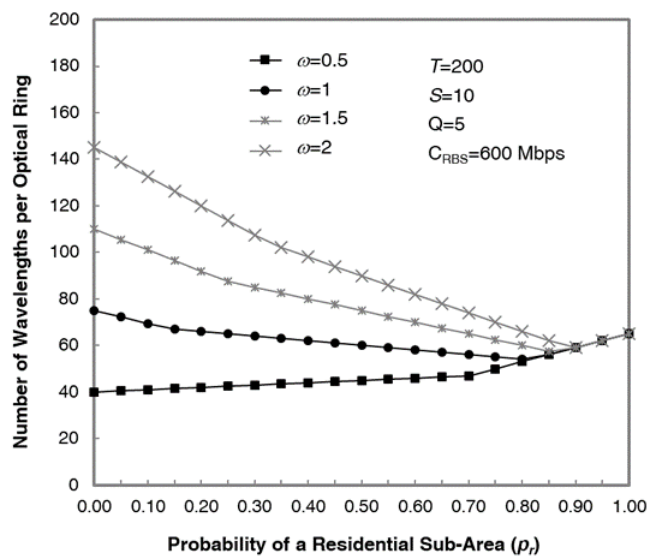


Figure 8. The number of wavelengths per optical ring is reported as a function of the probability p_r of residential sub-area. The peak offered traffic $A_{o,r}$ for a residential sub-area is fixed equal to 16 Gbps while the ratio $\omega = \frac{A_{o,b}}{A_{o,r}}$ is varied from 0.5 to 2. The percentage γ of used RRUs equals 0.6. $R = 2$ optical rings are considered. The values of the other parameters are chosen as the ones in Figure 5.

6. Featured Application

The main application of the proposed solution in this paper is in the 5G field. The transport network has a critical role to play in 5G by providing the backhaul and new fronthaul infrastructure that will enable all the interesting high bandwidth and ultra-low latency applications for millions of end devices. The separation of the remote radio unit (RRH) from the baseband unit (BBU) pools, dictated by 5G for supporting the high densification of the cells and the adoption of interference management procedures, is opening an uncharted territory in the 5G fronthaul network. The industry consensus is

that the physical medium for the 5G fronthaul network will be fiber. However, beyond this consensus point, there are many options being put forward and much debate including choice of transport protocols and even basic physical layer decisions for fiber. While promising solutions based on eCPRI and Ethernet technology are under investigation, we propose a feasible solution able to provide high bandwidth and dynamic resource allocation to lead high saving in realizing the transport network.

7. Conclusions

We have proposed an OTN/WDM network architecture to transport Ethernet and CPRI flows generated in a C-RAN. The network topology is composed of optical rings connecting Access Switches to an OTN/WDM Hub in which the baseband functionalities of a C-RAN are performed. The RRUs are equipped with active antennas and some MIMO configurations can be supported according to the traffic to be handled. An analytical model has been introduced to dimension the wavelengths of the rings when the Ethernet and CPRI circuits can be re-configured. We have shown how the introduced reconfiguration solution allows for a remarkable saving with respect to a static solution in which the optical rings are dimensioned to support the RBSs and RRUs when they work at full load. The wavelength saving can reach 90%. Finally we have shown how the proposed solution can be very effective when each AS handles the traffic generated by many sub-areas and the mix of business and residential user traffic, with peak average traffic in the PHI occurring in different stationary intervals.

Acknowledgments: The research has been supported by the project “Investigation of Trade-off between Power and Bandwidth Consumption in 5G Reconfigurable XHAUL Network Architecture” funded by University of Roma Sapienza.

Author Contributions: Vincenzo Eramo has organized and written the paper. Francesco Giacinto Lavacca has implemented the analytical model in Matlab language. Marco Listanti and Paolo Iovanna have provided useful comments for the results section.

Conflicts of Interest: The authors declare no conflict of interest.

Appendix A. Evaluation of the Probabilities of the Random Variable $N_{AS_{i,j},Eth}^k$

To evaluate the probabilities $p_{N_{AS_{i,j},Eth}^k}(j)$, we need to know the total traffic amount (Gbps) $A_{AS,E}^k$ expressed in Gbps and emitted by the RBSs handled by the sub-area $AS_{i,j}$. $A_{AS,E}^k$ is given by the sum of the traffic amount generated by the RBSs located in all of the sub-areas handled by $AS_{i,j}$. According to Assumption 4 in Section 4, all these components are independent and identically distributed (i.i.d.) with log-normal distributions of parameters $(\mu_k^{u,x}, \sigma_k^{u,x})$, being $x = b$ in the business case and $x = r$ in the residential case. In this case, it has been proven that the probability density $p_{A_{AS,E}^k}(x)$ of $A_{AS,E}^k$ can be approximated as log-normal probability density of parameters $(\mu_{AS,k}^{u,x}, \sigma_{AS,k}^{u,x})$ given by the following expressions [26]:

$$\sigma_{AS,k}^{u,x} = \sqrt{\log_e\left(\frac{1}{D}(e^{(\sigma_k^{u,x})^2} - 1) + 1\right)} \tag{A1}$$

$$\mu_{AS,k}^{u,x} = \log_e(De^{\mu_k^{u,x}}) + 0.5((\sigma_k^{u,x})^2 - (\sigma_{AS,k}^{u,x})^2) \tag{A2}$$

At this point, we can evaluate the probabilities $p_{N_{AS_{i,j},Eth}^k}(h)$ ($h = 1, \dots, \lceil Dn_{RBS}^x C_{RBS} \rceil$) from the probability densities $p_{A_{AS,E}^k}(h)$ of the random variable $A_{AS,E}^k$. We can simply write:

$$p_{N_{AS_{i,j},Eth}^k}(h) = \begin{cases} \frac{1}{2} \operatorname{erfc}\left(\frac{\mu_{AS,k}^{u,x}}{\sigma_{AS,k}^{u,x} \sqrt{2}}\right) & \text{if } h = 1 \\ \frac{1}{2} \operatorname{erfc}\left(-\frac{\log_e h - \mu_{AS,k}^{u,x}}{\sigma_{AS,k}^{u,x} \sqrt{2}}\right) - \frac{1}{2} \operatorname{erfc}\left(-\frac{\log_e (h-1) - \mu_{AS,k}^{u,x}}{\sigma_{AS,k}^{u,x} \sqrt{2}}\right) & \text{if } 2 \leq h \leq \lceil Dn_{RBS}^x C_{RBS} \rceil - 1 \\ 1 - \frac{1}{2} \operatorname{erfc}\left(-\frac{\log_e (\lceil Dn_{RBS}^x C_{RBS} \rceil - 1) - \mu_{AS,k}^{u,x}}{\sigma_{AS,k}^{u,x} \sqrt{2}}\right) & \text{if } h = \lceil Dn_{RBS}^x C_{RBS} \rceil \end{cases} \tag{A3}$$

Appendix B. Evaluation of Probabilities of the Events \mathcal{E}_{S_h} ($h = 0, \dots, Q - 1$)

For the evaluation of the probabilities $p_{S_h,k}^x$ ($h = 0, \dots, Q - 1; k = 0, \dots, N - 1; x \in \{b, r\}$) of the event \mathcal{E}_{S_h} , that is the probability that all of the RRUs of any sub-area apply the MIMO configuration S_h , we can make the following remarks:

- The event S_0 occurs when the traffic $A_k^{u,x}$ ($x \in \{b, r\}$ being $x = b$ in the business case and $x = r$ in the residential case) offered to the sub-area in the k -th SI is smaller than or equal to $n_{RBS}^x C_{RBS} + n_{RRU}^x C_0^{RRU}$, that is the total sum of the capacities of the n_{RBS} RBSs installed in the target sub-area and the capacity provided by the RRUs when they activate the MIMO configuration S_0 .
- The event S_h ($h = 1, \dots, Q - 2$) occurs when the traffic $A_k^{u,x}$ offered to the sub-area in the k -th SI is in the interval $[n_{RBS}^x C_{RBS} + n_{RRU}^x C_{h-1}^{RRU}, n_{RBS}^x C_{RBS} + n_{RRU}^x C_h^{RRU}]$.
- The event S_{Q-1} occurs when the traffic $A_k^{u,x}$ offered to the sub-area in the k -th SI is higher than $n_{RBS}^x C_{RBS} + n_{RRU}^x C_{Q-2}^{RRU}$.

According to the above observations, we can give the following expression for the probabilities $p_{S_h,k}^x$ ($h = 0, \dots, Q - 1; k = 0, \dots, N - 1$):

$$p_{S_h,k}^x = \begin{cases} \frac{1}{2} \operatorname{erfc}\left(-\frac{\log_e(n_{RBS}^x C_{RBS} + n_{RRU}^x C_0^{RRU}) - \mu_k^{u,x}}{\sigma_k^{u,x} \sqrt{2}}\right) & h = 0 \\ \frac{1}{2} \operatorname{erfc}\left(-\frac{\log_e(n_{RBS}^x C_{RBS} + n_{RRU}^x C_{i-1}^{RRU}) - \mu_k^{u,x}}{\sigma_k^{u,x} \sqrt{2}}\right) - \frac{1}{2} \operatorname{erfc}\left(-\frac{\log_e(n_{RBS}^x C_{RBS} + n_{RRU}^x C_i^{RRU}) - \mu_k^{u,x}}{\sigma_k^{u,x} \sqrt{2}}\right) & h = 1, \dots, Q - 2 \\ 1 - \frac{1}{2} \operatorname{erfc}\left(-\frac{\log_e(n_{RBS}^x C_{RBS} + n_{RRU}^x C_{Q-1}^{RRU}) - \mu_k^{u,x}}{\sigma_k^{u,x} \sqrt{2}}\right) & h = Q - 1 \end{cases} \quad (A4)$$

References

1. 5G-Oriented Optical Transport Network Solution. ZTE White Paper. Available online: <http://www.zte.com.cn/global/solutions/network/> (accessed on 15 February 2017).
2. Eramo, V.; Listanti, M.; Lavacca, F.G.; Iovanna, P.; Bottari, G.; Ponzini, F. Trade-Off Between Power and Bandwidth Consumption in a Reconfigurable Xhaul Network Architecture. *IEEE Access* **2016**, *4*, 9053–9065.
3. Velasco, L.; Castro, A.; Asensio, A.; Ruiz, M.; Liu, G.; Qin, C.; Proietti, R.; Yoo, S.J.B. Meeting the Requirements to Deploy Cloud RAN Over Optical Networks. *IEEE J. Opt. Commun. Netw.* **2017**, *9*, B22–B32.
4. Ranaweera, C.; Wong, E.; Nirmalathas, A.; Jayasundara, C.; Lim, Ch. 5G C-RAN with Optical Fronthaul: An Analysis from a Deployment Perspective. *IEEE J. Lightwave Technol.* **2017**, *99*, 1–11.
5. Alimi, I.A.; Teixeira, A.L.; Pereira Monteiro, P. Towards an Efficient C-RAN Optical Fronthaul for the Future Networks: A Tutorial on Technologies, Requirements, Challenges, and Solutions. *IEEE Commun. Surveys Tutor.* **2017**, *99*, 1–63.
6. Marotta, M.A.; Ahmadiy, H.; Rochol, J.; DaSilvaz, L.; Both, C.B. Characterizing the Relation between Processing Power and Distance between BBU and RRH in a Cloud RAN. *IEEE Wirel. Commun. Lett.* **2017**, *PP*, doi:10.1109/LWC.2017.2786226.
7. Eramo, V.; Listanti, M.; Lavacca, F.G.; Testa, F.; Sabella, R. Performance Evaluation of Integrated OTN/WDM Metropolitan Networks in Static and Dynamic Traffic Scenarios. *IEEE J. Opt. Commun. Netw.* **2015**, *7*, 761–775.
8. Iovanna, P.; Cavaliere, F.; Testa, F.; Stracca, S.; Bottari, G.; Ponzini, F.; Bianchi, A.; Sabella, R. Future Proof Optical Network, Infrastructure for 5G Transport. *IEEE J. Opt. Commun. Netw.* **2016**, *8*, B80–B92.
9. Lisi, S.S.; Alabbasi, A.; Tornatore, M.; Cavdar, C. Cost-Effective Migration towards C-RAN with Optimal Fronthaul Design. In Proceedings of the 2017 IEEE International Conference on Communications (ICC), Paris, France, 21–25 March 2017.
10. Mikaeil, A.M.; Hu, W.; Ye, T.; Hussain, S.B. Performance Evaluation of XG-PON Based Mobile Front-Haul Transport in Cloud-RAN Architecture. *IEEE J. Opt. Commun. Netw.* **2017**, *8*, 984–994.
11. Valcarenghi, L.; Kondepu, K.; Castoldi, P. Time- Versus Size-Based CPRI in Ethernet Encapsulation for Next Generation Reconfigurable Fronthaul. *IEEE J. Opt. Commun. Netw.* **2017**, *8*, D64–D73.

12. Elbers, J.P.; Zou, J.; Asimakopoulos, P.; Gomes, N.; Habel, K.; Jungnickel, V.; Linne, G.; Juchems, C.; Chanclou, P.; Ritosa, P.; et al. Next Generation Optical Fronthaul in the Project. In Proceedings of the Optical Fiber Communication Conference, San Diego, CA, USA, 11–15 March 2018.
13. Tayq, Z.; Le Guyader, B.; Chanclou, P.; Gosselin, S.; Abdourahmane, D.; Venmani, D.P.; Aupetit-Berthelemot, C.; Pachnicke, S.; Eiselt, M. Fronthaul Performance Demonstration in a WDM-PON-Based Convergent Network. In Proceedings of the 2016 European Conference on Networks and Communications (EuCNC), Athens, Greece, 27–30 June 2016.
14. CPRI Group. eCPRI Specification V1.0 and Requirements for the eCPRI Transport Network V1.1. Available online: <http://www.cpri.info/> (accessed on 3 April 2018).
15. Eramo, V.; Listanti, M.; Lavacca, F.G.; Iovanna, P.; Bottari, G.; Ponzini, F. Bandwidth Saving in Xhaul Network Architecture with CPRI Line Bit Rate Reconfiguration. In Proceedings of the 2017 19th International Conference on Transparent Optical Networks (ICTON), Girona, Spain, 2–6 July 2017.
16. Eramo, V.; Listanti, M.; Sabella, R.; Testa, F. Definition and Performance Evaluation of a Low-Cost/High-Capacity Scalable Integrated OTN/WDM Switch. *IEEE J. Opt. Commun. Netw.* **2012**, *4*, 1033–1045.
17. Eramo, V.; Listanti, M.; Sabella, R.; Testa, F. Integrated OTN/WDM Switching Architecture Equipped With the Minimum Number of OTN Switches. *IEEE J. Opt. Commun. Netw.* **2014**, *6*, 138–151.
18. Li, G.; Creazzo, T.; Marchena, E.; Yu, P.K.L.; Krasulick, S. A CMOS wafer-scale, monolithically integrated WDM platform for TB/s optical interconnects. In Proceedings of the 2014 Optical Fiber Communications Conference and Exhibition (OFC), San Francisco, CA, USA, 9–14 March 2014.
19. Duan, G.H.; Jany, C.; Le Liepvre, A.; Accard, A.; Lamponi, M.; Make, D.; Kaspar, P.; Levaufre, G.; Girard, N.; Lelarge, F.; et al. Hybrid III-V on silicon lasers for photonic integrated circuits on silicon. *IEEE J. Sel. Top. Quantum Electron.* **2014**, *20*, 158–170.
20. Lee, D.; Zhou, S.; Zhong, X.; Niu, Z.; Zhou, X.; Zhang, H. Spatial modeling of the traffic density in cellular networks. *IEEE Wirel. Commun.* **2014**, *21*, 80–88.
21. The New Ethernet-Driven OTN. *Fujitsu*. Available online: <https://www.fujitsu.com/us/Images/EthDrivenOTNwp.pdf> (accessed on 15 February 2017).
22. OTN Transport of CPRI Signals. ITU-T G-Series Recommendations-Supplement 56. Available online: <https://www.itu.int/rec/T-REC-G.Sup56/en> (accessed on 15 February 2018).
23. Checko, A.; Holm, H.; Christiansen, H. Optimizing small cell deployment by the use of C-RANs. In Proceedings of the 2014 20th European Wireless Conference, Barcelona, Spain, 14–16 May 2014.
24. Checko, A.; Christiansen, H.; Yan, Y. Cloud RAN for Mobile Networks: A Technology Overview. *IEEE Commun. Surveys Tutor.* **2014**, *17*, 405–426.
25. CPRI Group. CPRI Specification V7.0; Common Public Radio Interface (CPRI): Interface Specification. Available online: <http://www.cpri.info/> (accessed on 3 April 2018).
26. Cobb, B.R.; Salmeron, R.R.A. Approximating the distribution of a sum of log-normal random variables. In Proceedings of the 6th European Workshop on Probabilistic Graphical Models, Granada, Spain, 6–8 November 2012.

